Short communication

Supercapacitive properties of hybrid films of manganese dioxide and polyaniline based on active carbon in organic electrolyte

Wu-yuan Zou, Wei Wang*, Ben-lin He, Ming-liang Sun, Yan-sheng Yin

Institute of Materials Science and Engineering, Ocean University of China, Songling Road 238, Qingdao 266100, Shandong Province, PR China

ARTICLE INFO

ABSTRACT

This is the first report about supercapacitive performance of hybrid film of manganese dioxide (MnO_2) and polyaniline (PANI) in an organic electrolyte (1.0 M $LiClO_4$ in acetonitrile). In this work, a high surface area and conductivity of active carbon (AC) electrode is used as a substrate for PANI/MnO_2 film electro-codeposition. The redox properties of the coated PANI/MnO_2 thin film exhibit ideal capacitive behaviour in 1 M $LiClO_4$/AN. The specific capacitance (SC) of PANI/MnO_2 hybrid film is as high as 1292 F g^{-1} and maintains about 82% of the initial capacitance after 1500 cycles at a current density of 4.0 mA cm^{-2}, and the coulombic efficiency (η) is higher than 95%. An asymmetric capacitor has been developed with the PANI/MnO_2/AC positive and pure AC negative electrodes, which is able to deliver a specific energy as high as 61 Wh kg^{-1} at a specific power of 172 W kg^{-1} in the range of 0–2.0 V. These results indicate that the organic electrolyte is a promising candidate for PANI/MnO_2 material application in supercapacitors.

© 2010 Elsevier B.V. All rights reserved.

1. Introduction

The performances of supercapacitors are mainly determined by electrode materials [1]. Conducting polymers and inorganic particle composite materials have attracted considerable attention as they can combine the advantages of their separate components and have potential applications in many fields [2]. Research of composite materials in supercapacitors for electrode materials has been undertaken by many researchers in recent years [3–10].

Polyaniline (PANI) is one candidate for supercapacitors due to its electrochemical reversibility and stability [11]. Manganese oxides are also promising supercapacitor materials due to their low cost and the fact that manganese oxides are considered more environmental friendly than other transition metal oxide systems [12,13]. The composite of polyaniline and manganese oxides can be achieved by chemical or electrochemical polymerization [14–17]. Unfortunately, most studies on PANI/MnO_2 composite electrodes for supercapacitor applications reported in the literature [13–17] have focused on the use of aqueous electrolytes whose major drawback lies in its low cell voltage. For example, Sun et al. [16,17] studied the capacitive properties of PANI/MnO_2 hybrid films in 1.0 M $NaNO_3$ (pH = 1) only with a window of 0.65 V applied potential. In that case, the PANI/MnO_2 composite electrodes usually show a quite low energy density according to the calculation equation [18].

Generally, the stability of electrode materials will decrease drastically with an increase in the potential window. Under a high applied potential window, if the PANI/MnO_2 hybrid films could improve the stability and show a higher specific capacitance in an electrolyte, it means that this electrolyte is a suitable candidate for PANI/MnO_2 material application in supercapacitors. For this purpose, this work will be devoted to an investigation of the supercapacitive performance of PANI/MnO_2 composites in 1 M $LiClO_4$/AN electrolyte. To the best of our knowledge, this study has not been reported yet. We prepared the nanocomposite thin film of PANI/MnO_2 codeposited on an active carbon (AC) substrate since a high surface area of carbon substrate will be propitious to enhance the total conductivity and stability of the composite electrode [19,20]. In addition, the asymmetric capacitor was assembled with the PANI/MnO_2/AC positive and pure AC negative electrodes.

2. Experimental

2.1. Preparation of active carbon (AC) electrode

Activated carbon powders serving as the main electrode materials (specific surface area: >2000 m^2 g^{-1}) and an amount of conductive acetylene black were added to a solution of polyvinylidenefluoride (PVDF) in N-methyl-pyrrolidone (NMP). The mixture was stirred at about 170 °C to form the carbon slurry. Carbon electrodes (1 cm × 1 cm square) were fabricated by coating the slurry on stainless steel nets, which were subsequently dried at 80 °C for 24 h to remove the NMP.

2.2. Preparation of PANI/MnO₂/AC and PANI/AC composite electrodes

The synthesis of PANI/MnO$_2$ thin films was done in a simple method. Briefly, electrodepositions of PANI/MnO$_2$ hybrid films were produced simultaneously on the active carbon substrate electrodes through CV in the potential range of −0.2 to 1.45 V (vs. Ag/AgCl) at 50 mV s^{-1}, from solutions of 0.4 M aniline and 0.1 M MnSO$_4$, containing 0.5 M H$_2$SO$_4$. The PANI film was deposited similarly in 0.5 M H$_2$SO$_4$ containing 0.4 M aniline. The preparation of all samples was conducted under a nitrogen atmosphere.

2.3. Characterization

Electrochemical tests were carried out within a three-compartment cell with the PANI/MnO$_2$/AC or AC as the working electrode, using a platinum foil ($A = 1.0$ cm^2) as the counter-electrode, and Ag/AgCl being the reference electrode. The asymmetric hybrid capacitor was assembled with PVDF-HFP separator and 1 M LiClO$_4$ in acetonitrile (AN) electrolyte. A symmetric capacitor containing two identical pure AC electrodes was also fabricated under the same condition. CV tests were realized on the LK9805Z electrochemical workstation system (Lanlike Company, Tianjin). The galvanostatic charge–discharge experiments were conducted on the battery test system (Land CT2001A, Wuhan, China). The microstructure of the samples was characterized using a scanning electron microscope (SEM, JSM-6700F Japan). XRD measurements were performed on Bruker AXS D8 Advance.

3. Results and discussion

3.1. Characterization of AC, PANI/AC and PANI/MnO₂/AC

Surface morphologies of PANI/MnO$_2$ hybrid films, bare electrodes (AC), and PANI films are investigated by SEM (Fig. 1). The surface morphologies of AC electrodes are rough and porous due to the intrinsic nature of the activated carbon substrate (Fig. 1(A)). Fig. 1(B) shows nanofibrous morphology for PANI/AC, which is the evidence of PANI deposition on AC substrate. For PANI/MnO$_2$/AC (Fig. 1(C)), the PANI nanofibers are coated by a mass of particles and the diameter of fibers is larger than that of pure PANI fibers, which suggests the codeposition of MnO$_2$ with the growth of PANI on the AC substrate. The EDS analysis of PANI/MnO$_2$/AC (Fig. 1(D)) indicates the existence of Mn, O and C species in the composites, which should be attributable to the MnO$_2$ and PANI phases. The PANI/MnO$_2$ films on the AC electrode present a large amount of fibers with diameters of 100–200 nm in the mass and the fibers inter-twine together to form a three-dimensional reticulation. Such porous microstructure would be an ideal candidate as electrode material for supercapacitors since it has more available active sites for faradic reaction and is also favorable for charge-transfer.

Fig. 2 shows powder X-ray diffraction patterns of samples. For PANI (Fig. 2(b)), the crystalline peaks appeared at 14.9°, 20.6°, 25.5°, corresponding, respectively, to (0 1 1), (0 2 0) and (2 0 0) reflections of PANI in its emeraldine salt form [21]. The peaks of 22.5° and 28.5° are attributable to the AC substrate (Fig. 2(a)), which is indicative of its high electrical conductivity. Compared with PANI, there are no distinguished XRD peaks in the hybrid film (Fig. 2(c)), revealing the amorphous nature of MnO$_2$ in the composites. Brousse et al. [22] have reported that amorphous MnO$_2$ can be seen to contain inter-growth of different tunnel structures which should be convenient for cation diffusion. Subsequently, this can translate into a large scattering of capacitance values not based only upon the surface area but also on the structural disorder of the samples.
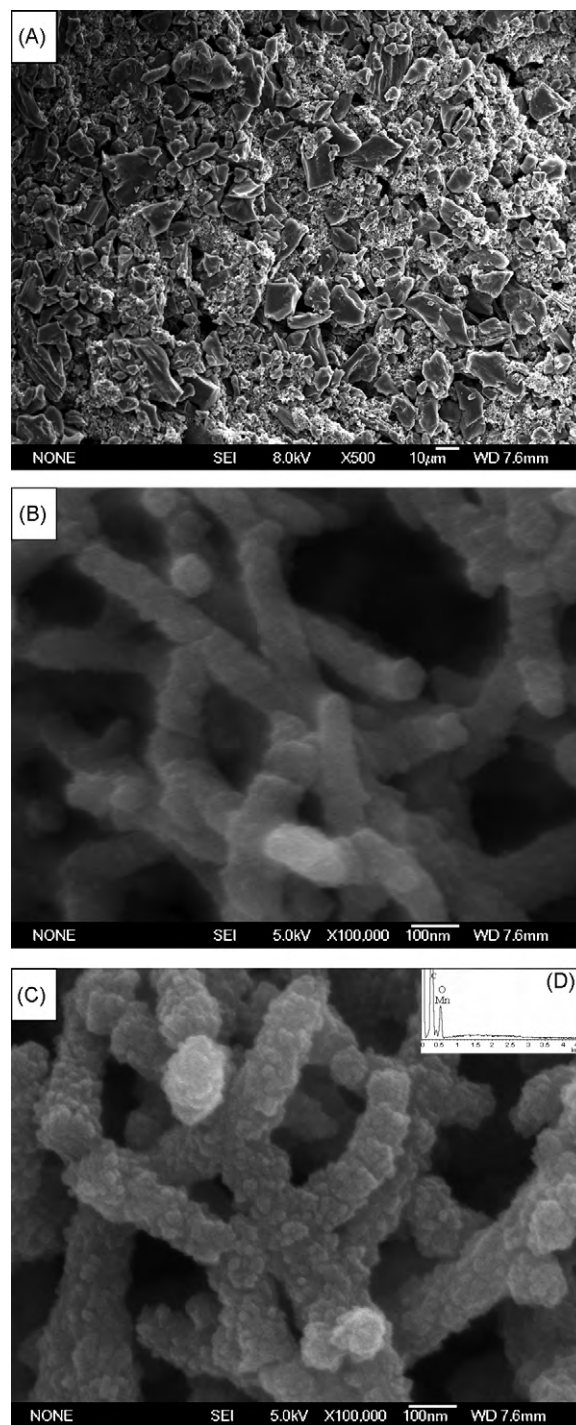

Fig. 1. SEM morphologies of AC (A), PANI/AC (B), PANI/MnO$_2$/AC (C), and EDS of PANI/MnO$_2$/AC (D).

3.2. Supercapacitive properties of PANI/MnO₂/AC

The PANI/MnO$_2$/AC nanocomposites are tested using the method of potential sweep in 1 M LiClO$_4$/AN to study the supercapacitive properties. Fig. 3 shows the CV curve of the AC and PANI/MnO$_2$/AC electrode. The CV curve of the substrate electrode is in the nature of a double layer capacitor, while the PANI/MnO$_2$/AC shows the pseudocapacitive behaviour [23]. Theoretically, the pure PANI and MnO$_2$ material should have an obvious redox characteristic [24,25]. However, in our case, the redox peaks are not clear in Fig. 3. The possible reasons may be: (I) the highly disor-
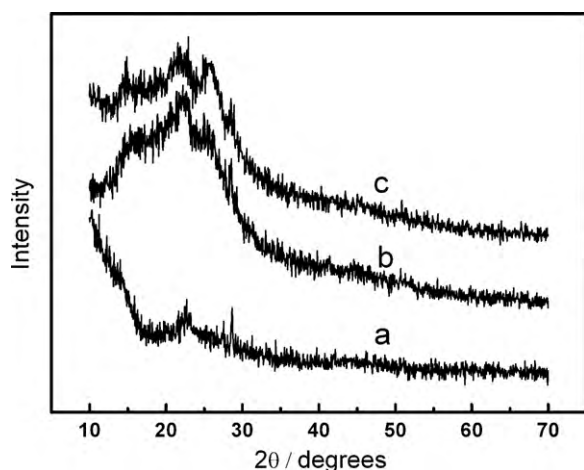
Fig. 2. XRD patterns of AC (a), PANI/AC (b) and PANI/MnO$_2$/AC (c).

Fig. 4. CV tests of PANI/MnO$_2$/AC electrode at 1 mV s^{-1} (a), 2 mV s^{-1} (b), and 5 mV s^{-1} (c) in 1 M LiClO$_4$/AN electrolyte.

dered structure of the electrodeposited amorphous MnO$_2$ in the PANI/MnO$_2$/AC electrode [18,26,27]; (II) low levels of MnO$_2$ in the nanocomposite electrode (only 0.95% by EDS analysis); (III) a more positive potential (>0.8 V) would accelerate the degradation of PANI on the polymerization [28,29]. This results in a decrease of activity on the chains of PANI.

Fig. 4 shows the CV curves of PANI/MnO$_2$/AC at various scan rates. During potential cycling, the increase of scan rate usually has a negative impact on the pseudocapacitance of the working electrode [4]. However, when increasing the scan rate from 1 to 5 mV s^{-1}, the CV shapes comparatively little change and all the CV curves show near ideal rectangular image, which indicates the good pseudocapacitive behaviour. This capacitive nature may be caused by combining the double layer capacitance of AC substrates and the pseudocapacitance of PANI/MnO$_2$ film [13].

The SC of the electrodes is estimated by CV. A 187 and 413 F g^{-1} are achieved for pure AC electrode and PANI/MnO$_2$/AC electrode with the high applied potential of 1.2 V. The values of SC and potential window are higher than the literature results in aqueous electrolyte [13,14]. Based on the combined mass of AC, PANI and MnO$_2$ phases, the SC of 413 F g^{-1} for this nanocomposite electrode is even impressive in an organic electrolyte, especially under a high potential window.

Fig. 5(A) illustrates the typical charging–discharging behaviours of the PANI/MnO$_2$/AC hybrid electrode recorded in 1 M LiClO$_4$/AN.
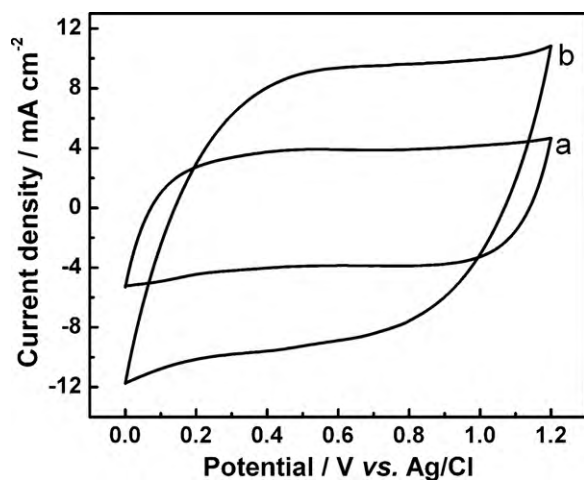
The curve shows an almost linear decline of potential between the operating voltages 0 and 1.2 V, which is the characteristic of capacitive behaviour. The SC of the nanocomposite electrode was calculated from the discharge profile. The value of SC is 408 F g^{-1} at a current density of 4.0 mA cm^{-2}, which is very close to the calculated results of CV. The SC of the coated PANI/MnO$_2$ thin film can

Fig. 5. (A) Charging–discharging curves of PANI/MnO$_2$/AC electrode at 4.0 mA cm^{-2} in 1 M LiClO$_4$/AN electrolyte; (B) variation of specific capacitance and coulombic efficiency with charging–discharging cycle number for PANI/MnO$_2$/AC at 4.0 mA cm^{-2} in 1 M LiClO$_4$/AN electrolyte.

Fig. 3. CV tests of AC electrode and PANI/MnO$_2$/AC electrode in 1 M LiClO$_4$/AN electrolyte at 5 mV s^{-1} (a: AC and b: PANI/MnO$_2$/AC).
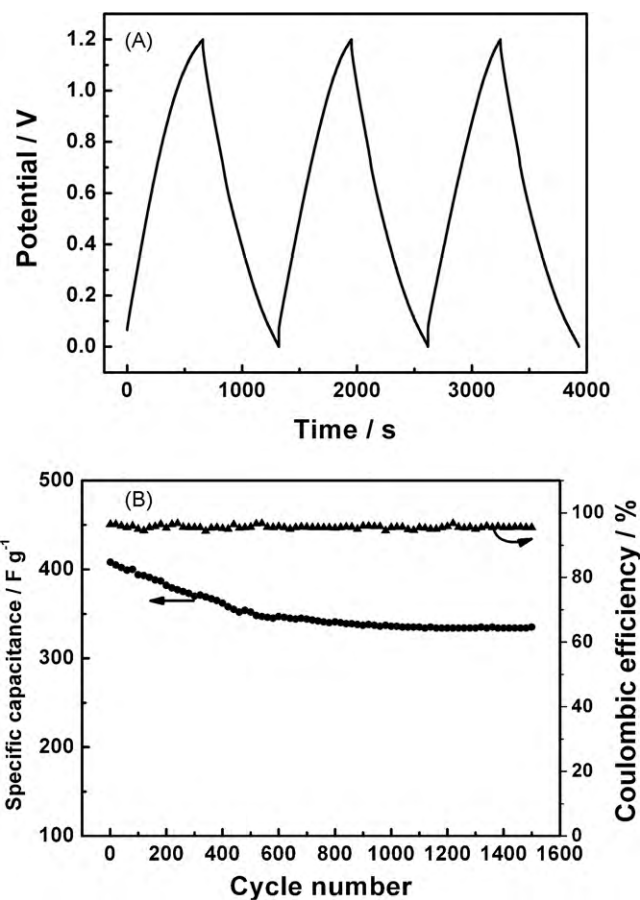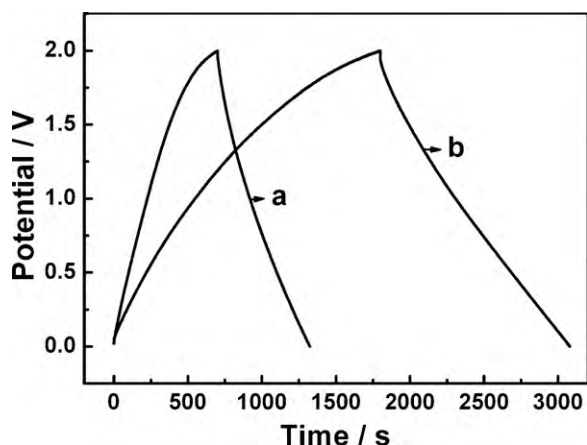
Fig. 6. First charge/discharge profiles of the hybrid capacitor at 0.17 A g^{-1}. (a) Symmetric capacitor containing two identical pure AC electrodes; (b) asymmetric capacitor using PANI/MnO$_2$/AC and AC as the positive and negative electrode, respectively.

be calculated based on the following equation:

$$C_{\text{PANI/MnO}_2} = \frac{C_{\text{hybrid}} - C_{\text{substrate}}}{M_{\text{PANI/MnO}_2}} \qquad (1)$$

where $C_{\text{PANI/MnO}_2}$, C_{hybrid}, $C_{\text{substrate}}$ and $M_{\text{PANI/MnO}_2}$ are the SC of PANI/MnO$_2$ composite film, PANI/MnO$_2$/AC composite electrode, pure AC substrate electrode and the mass of PANI/MnO$_2$ film, respectively. The SC of coated PANI/MnO$_2$ was as high as 1292 F g^{-1} at a voltage window of 1.2 V. This value is far higher than that of these papers [13,14,16,17,25]. Out of question, the energy density of this PANI/MnO$_2$ film has the same conclusion.

Furthermore, the composites display a sustained cyclic ability, while being subjected to 1500 charge/discharge cycles at a current density of 4.0 mA cm^{-2}. The variation of specific capacitance as a function of cycle number is shown in Fig. 5(B). A capacity fade of just 18% was observed after 1500 charge/discharge cycles, which is better than the previous report, indicating the high stability of PANI/MnO$_2$/AC nanocomposite and its potential as an electrode material for long-term capacitor applications in such organic electrolytes. The explanation of these results can be as following: (1) the MnO$_2$ particle clusters in the polymer matrix essentially provide rigid support for the stability of the PANI chains during redox cycling. (2) Hydrolytic reaction of PANI disappeared under an organic environment, which greatly retards the degradation of PANI [23,30]. (3) The reversible intercalation/deintercalation of Li$^+$ in the MnO$_2$ solid phase, which can be ascribed to the small radius of the Li$^+$ and poorly crystallized MnO$_2$ [22]. (4) The high conductivity of the AC substrates. (5) The PANI/MnO$_2$ film was homogeneously coated on the porous AC surface and the film was quite thin.

The coulombic efficiency (η) of the PANI/MnO$_2$/AC is also shown in Fig. 5(B). The result reveals that the nanocomposite electrode has a very stable coulombic efficiency of about 95.5% over 1500 cycles.

In order to further investigate the supercapacitive performance of PANI/MnO$_2$ hybrid material under a higher potential, an asymmetric capacitor, respectively using PANI/MnO$_2$/AC nanocomposite and AC as the positive and negative electrode materials was assembled. For comparison purpose, a symmetric capacitor containing two identical pure AC electrodes was also fabricated. Fig. 6 shows the first charge/discharge profiles of the capacitor cells. The charge/discharge cycle for the cell was performed in 1 M LiClO$_4$/AN at a constant current of 0.17 A g^{-1} between 0 and 2.0 V. The discharge profiles of the asymmetric and symmetric capacitor show a typical capacitive behaviour with a linear slope. These results accord with Fig. 3. The specific energy (E) and power (P) were calculated by following equations from the constant current charge/discharge cycle:

$$E = \frac{1}{2}CV^2 (\text{Wh kg}^{-1}) \qquad (2)$$

$$P = \frac{E}{t} (\text{W kg}^{-1}) \qquad (3)$$

where C is the specific capacitance of the hybrid capacitor, V is the potential range from the end of the charge to the end of the discharge and t is the discharge time. Using these equations, the specific energy of the asymmetric capacitor is 61 Wh kg^{-1} at a specific power of 172 W kg^{-1} based on the total weight of AC and PANI/MnO$_2$/AC nanocomposite, while the symmetric capacitor shows a 31 Wh kg^{-1} at a specific power of 179 W kg^{-1} according to the weight of active material in both electrodes. The specific power of symmetric capacitor is slightly higher than the asymmetric capacitor, which can be explained on basis of the nature of electrical double layer in AC electrode. But the specific energy of the latter is expected to show ∼2 times higher than the former. This result reveals the asymmetric capacitor containing PANI/MnO$_2$ positive material show a great capacitor performance using organic electrolyte.

4. Conclusion

In this study, a hybrid thin film of PANI/MnO$_2$ with nanofibrous morphologies was electro-codeposited on an AC substrate. The electrochemical properties of this PANI/MnO$_2$/AC electrode were examined in 1 M LiClO$_4$/AN. This is the first attempt to research the performance of PANI/MnO$_2$ hybrid film in organic electrolyte. At a current density of 4.0 mA cm^{-2}, the coated PAN/MnO$_2$ film could produce SC as high as 1292 F g^{-1} and the composite electrode showed a capacity fade of only 18% after 1500 cycles. The specific energy of asymmetric capacitor which consists of PANI/MnO$_2$/AC positive and AC negative electrodes was 61 Wh kg^{-1} at a specific power of 172 W kg^{-1}. These results indicated that the nonaqueous organic electrolyte is suitable for PANI/MnO$_2$ hybrid material to apply in supercapacitors.

References

[1] J.P. Zheng, P.J. Cygan, T.R. Jow, J. Electrochem. Soc. 142 (1995) 2699.
[2] X.X. Liu, L.J. Bian, L. Zhang, L.J. Zhang, J. Solid State Electrochem. 11 (2007) 1279.
[3] M. Biswas, S.S. Ray, Y.P. Liu, Synth. Met. 105 (1999) 99.
[4] R.K. Sharma, A.C. Rastogi, S.B. Desu, Electrochim. Acta 53 (2008) 7690.
[5] A.H. Gemeay, I.A. Mansour, R.G. El-Sharkawy, A.B. Zaki, Eur. Polym. J. 41 (2005) 2575.
[6] S.C. Canobre, L. Montanhez, C.P. Fonseca, S. Neves, Mater. Chem. Phys. 114 (2009) 350.
[7] M. Malta, R.M. Torresi, Electrochim. Acta 50 (2005) 5009.
[8] S. Neves, S.C. Canobre, R.S. Oliveira, C.P. Fonseca, J. Power Sources 189 (2009) 1167.
[9] F.J. Liu, J. Power Sources 182 (2008) 383.
[10] A.K. Cuentas-Gallegos, P. Gomez-Romero, J. Power Sources 161 (2006) 580.
[11] S. Mu, C. Chen, J. Wang, Synth. Met. 88 (1997) 249.
[12] R.N. Reddy, R.G. Reddy, J. Power Sources 124 (2003) 330.
[13] Z.H. Zhou, N.C. Cai, Y.H. Zhou, Mater. Chem. Phys. 94 (2005) 371.
[14] C.Z. Yuan, L.H. Su, B. Gao, X.G. Zhang, Electrochim. Acta 53 (2008) 7039.
[15] X. Zhang, L.Y. Ji, S.C. Zhang, W.S. Yang, J. Power Sources 173 (2007) 1017.
[16] L.J. Sun, X.X. Liu, K.K-T. Lau, L. Chen, W.M. Gu, Electrochim. Acta 53 (2008) 3036.
[17] L.J. Sun, X.X. Liu, Eur. Polym. J. 44 (2008) 219.
[18] K.W. Nam, C.W. Lee, X.Q. Yang, B.W. Cho, W.S. Yoon, K.B. Kim, J. Power Sources 188 (2009) 323.
[19] M. Sipahi, E.A. Parlak, A. Gul, E. Ekinci, M.F. Yardim, A.S. Sarac, Prog. Org. Coat. 62 (2008) 96.

[20] S.K. Mondal, K. Barai, N. Munichandraiah, Electrochim. Acta 52 (2007) 3258.
[21] B. Dong, B.L. He, C.L. Xu, H.L. Li, Mater. Sci. Eng. B 143 (2007) 7.
[22] T. Brousse, M. Toupin, R. Dugas, L. Athouë, O. Crosnier, D. Bélanger, J. Electrochem. Soc. 153 (2006) A2171.
[23] S.B. Ma, K.W. Nam, W.S. Yoon, X.Q. Yang, K.Y. Ahn, K.H. Oh, K.B. Kim, Electrochem. Commun. 9 (2007) 2807.
[24] B. Garcia, F. Fusalba, D. Bélanger, Can. J. Chem. 75 (1997) 1536.
[25] K.R. Prasad, N. Miura, J. Electrochem. Soc. 7 (2004) A425.
[26] M.M. Thackeray, Prog. Solid State Chem. 25 (1997) 1.
[27] J.J. Xu, J. Yang, Electrochem. Commun. 5 (2003) 230.
[28] T. Kobayashi, H. Yoneyama, H. Tamura, J. Electroanal. Chem. 177 (1984) 293–297.
[29] A.A. Pud, Synth. Met. 66 (1994) 1–18.
[30] A.A. Hathoot, Bull. Kor. Chem. Soc. 24 (2003) 1609.